ELSEVIER

Journal of Non-Crystalline Solids 274 (2000) 81–86

JOURNAL OF NON-CRYSTALLINE SOLIDS

www.elsevier.com/locate/jnoncrysol

Section 5. Glass structure III

Glass structure and light scattering

B. Champagnon *, C. Chemarin, E. Duval, R. Le Parc

Laboratoire de Physico–Chimie des Matériaux Luminescents, Campus La Doua, UMR 5620 CNRS Université Lyon 1, 69622 Villeurbanne cedex, France

Abstract

Elastic and inelastic light scattering experiments are performed on silica, SiO_2, with OH content < 20 ppm. Quantitative comparison is made between Raman, Brillouin and Rayleigh scattered intensities showing that for an accurate comparison Raman scattering has to be considered. The decrease of the Rayleigh scattering and the shift of the Boson peak with the decrease of the fictive temperature are attributed to two types of inhomogeneities typical of the structure of glass: frozen density fluctuations and elastic constant fluctuations in domains with dimensions $\sim$1 nm.

1. Introduction

The structure of simple glasses is still a debated question [1–3]. Cation correlations, characteristic lengths, domains, clusters, with a typical size in the nanometer range are often proposed to interpret experimental results or computer simulations. Inelastic light scattering experiments in the low frequency domain (Boson peak) are interpreted [4–7] as being due to inhomogeneities in the structure of the glass but these models are still a matter of discussion. Besides, elastic scattering (Rayleigh scattering) in a simple component glass such as SiO_2 [8] is well interpreted as due to density fluctuations.

In recent papers, we demonstrated the role of thermal treatment on the energy of the Boson peak [5,6]. Simultaneously, several papers [9–12] investigated Rayleigh scattering and its relation to fictive temperature. These experiments, however, do not study the elastic scattering but both elastic and inelastic scattering as no dispersive element is used to analyze the scattered light.

In this paper, we will make the spectral analysis of scattering to separate the different contributions of Rayleigh, Brillouin, and Raman processes. We propose further to follow their evolution with the fictive temperature to correlate these observations with the structure of the glass.

2. Experiments and materials

Spectral analysis of light scattering is usually performed by two kind of dispersive devices. Inelastic Raman scattering is studied with a double or a triple monochromator, whereas measurements of elastic (Rayleigh) and much lower frequency inelastic (Brillouin) scatterings are made with a Fabry–Perot interferometer. In this work, we performed both elastic and inelastic scatterings with a five stage monochromator (Dilor

* Corresponding author. Tel.: +33-4 72 44 83 34; fax: +33-4 72 44 84 42.

E-mail address: champ@pcml.univ-lyon1.fr (B. Champagnon).

0022-3093/00/$ - see front matter
PII: S0022-3093(00)00207-6

Z40). The conception of this system, where six slits filter the scattered light before the photomultiplier, is rejection of the input light as much as possible which allows us to record both Rayleigh and Brillouin and full anti-Stokes and Stokes Raman Scattering with the same experimental set-up. A neutral filter (optical density $D = 4$) is placed in the scattered beam at the laser frequency during scanning of the spectrometer. These experiments are done with an argon laser with the 514 nm line in a 90° configuration, the spectra reported in this paper are all made in parallel VV polarizations for the incident and scattered light. Samples are silica glasses with OH content less than 20 ppm. As-received sample is measured (sample A) together with a sample annealed for 1 h at 1200°C (sample B), 18 h at 1150°C (sample C) and 60 h at 1100°C (sample D) to achieve different fictive temperatures. Samples, with a typical thickness 5 mm, were cooled on a metallic plate.

3. Results

Several methods exist to determine the fictive temperature of a silica glass, based on the shift of the IR absorption line at 2250 cm^{-1} in transmission or 1120 cm^{-1} in reflection [13], or on the relative intensities of the D_1 and D_2 defect lines at 490 cm^{-1} and 606 cm^{-1}, respectively [14]. We analyzed the Raman spectra of the four samples. The slope of the log of intensity as functions of $1/T_F$ is larger for the D_2 lines and allows better accuracy for the determination of T_F (Fig. 1).

The Brillouin and Rayleigh scatterings of sample A are shown in Fig. 2 using entrance and exit slits of 30 μm. The spectra for the samples A, B, D are also recorded with larger slits (300 μm): the spectra integrating Rayleigh and Brillouin scatterings from −3 to +3 cm^{-1} (Fig. 3) and the whole Raman spectrum from −600 to 1200 cm^{-1} (Fig. 4). The neutral filter was used for Fig. 3 and for the scan between −10 and 10 cm^{-1} of Fig. 4.

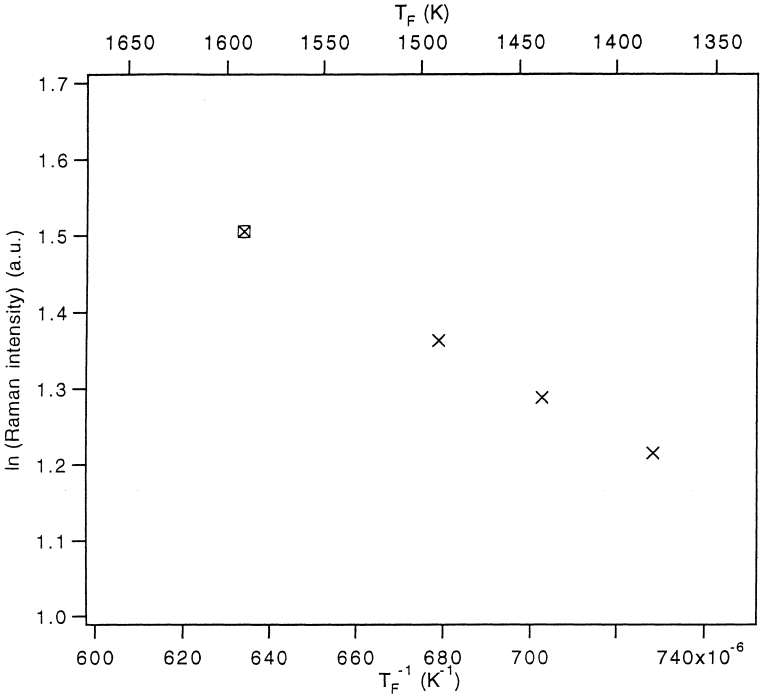

Fig. 1. Log of the Raman intensity of the D_2 line as function of the inverse of the fictive temperature, T_F. The extrapolation of the curve to higher intensity gives the fictive temperature of the sample A (□).

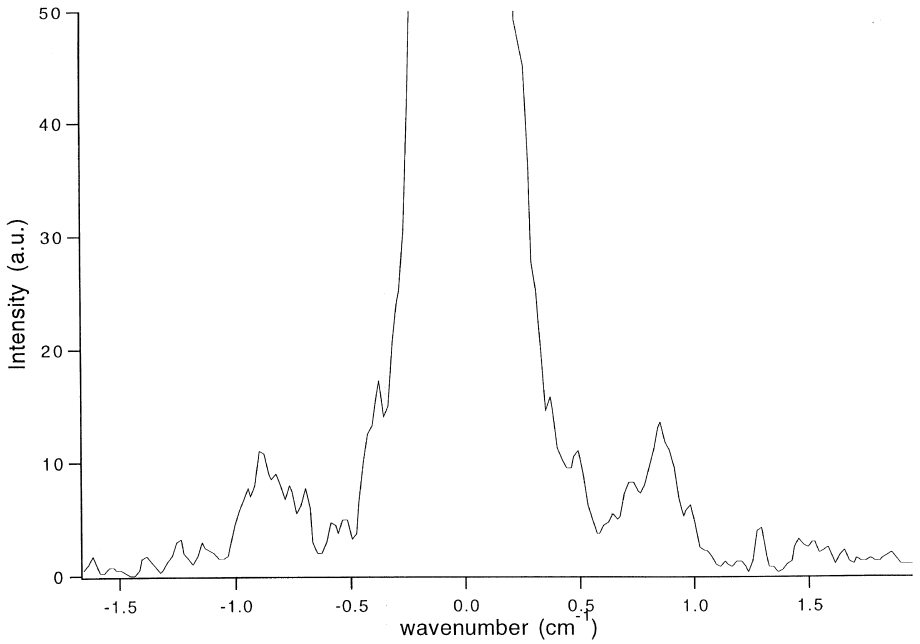

Fig. 2. Rayleigh and Brillouin scattering for the sample. A recorded with the Z40 monochromator (slit width 50 μm).

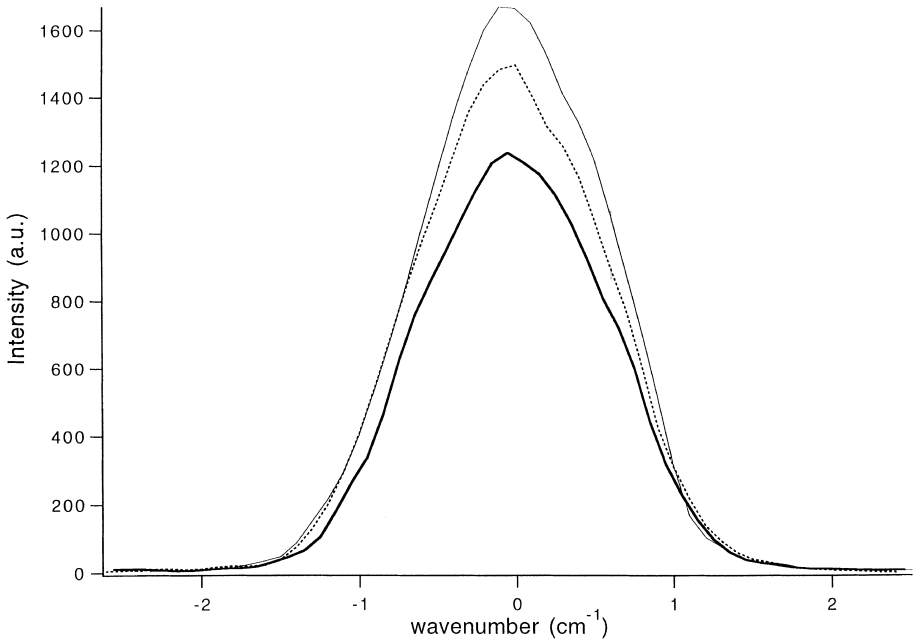

Fig. 3. Integrated Rayleigh and Brillouin scattering for the samples sample A (), B (· · · · · · · · ·), and D (——) (slit width 300 μm).

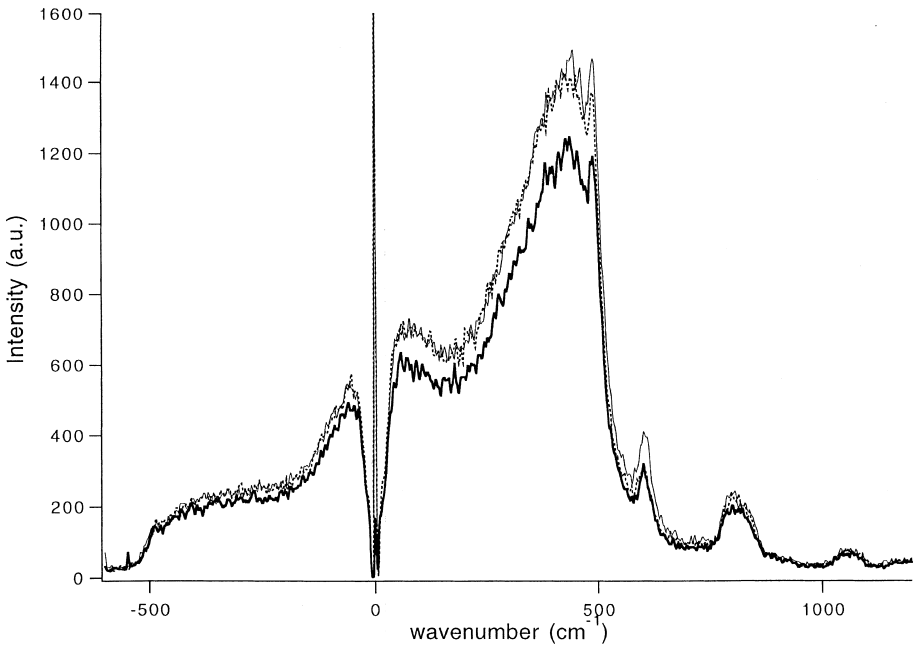

Fig. 4. Raman spectra of the sample A (), B (·····), and D (—) from −600 to 1200 cm^{-1}.

4. Interpretation and discussion

4.1. Fictive temperature

Annealing times for the samples treated at 1100°C, 1150°C and 1200°C are long enough [9] to achieve equilibrium of the structure corresponding actually to fictive temperature 1100°C, 1150°C and 1200°C. The fictive temperature of the sample A can be estimated from a Galeener plot (Fig. 1). Linear extrapolation of this plot leads to an estimate of the fictive temperature of sample A: $T_f = 1304 \pm 20$°C.

4.2. Elastic and inelastic scattering

The decrease of the Rayleigh scattering when the fictive temperature decreases is shown in Fig. 3. This decrease is in agreement with the interpretation of the elastic scattering as being due to density fluctuations 'frozen' at T_F. The Rayleigh intensity, $I_{Rayleigh}$, is then proportional to the mean square amplitude of density fluctuations, $\langle|\Delta\rho|^2\rangle$ [8,9]

$$I_{\text{Rayleigh}} \propto \langle|\Delta\rho|^2\rangle \propto \frac{8\Pi^3 k_B}{3\lambda^4} n^8 p^2 K_T(T_F) T_F, \quad (1)$$

where n is the refractive index, p the photoelastic constant, K_T (T_F) is the isothermal compressibility at T_F. The relation between $I_{Rayleigh}$ and T_F is linear only in a first approximation, where n and K_T dependence on T_F are neglected. This point will be explored in further experiments involving a larger number of samples. However, from our measurements, the decrease of the fictive temperature from 1304°C to 1100°C decreased the Rayleigh scattering by $15 \pm 2\%$, in agreement with a linear relation taking into account the experimental error both on the temperature and on the Rayleigh intensity.

Fig. 4 shows the Raman spectra of the samples A, B and D, which represent approximately 3% of the total scattering of the samples taking into account both Stokes and anti-Stokes scattering. The decrease of the intensity observed with decrease of T_F is still to be experimentally confirmed but it emphasizes that, even if the variation of scattering is mainly due to the Rayleigh process, for a precise determination, Raman scattering also has to be considered.

The optical loss, α_S, usually determined from the measured Landau–Placzek ratio, R_{LP} [7], of the Rayleigh, $I_{Rayleigh}$, to the Brillouin lines, $2I_B$, as obtained from Fig. 3 is given by

$$\alpha_S = \frac{8\Pi^3}{3}\frac{k_B T}{\lambda^4} n^8 p^2 \frac{1}{\rho v}(R_{LP}+1),$$

ρ being the density and v the sound velocity of the samples. For sample D, we determined $R_{LP} = 23.0$, which corresponds to

$$R_{LP}+1 = \frac{2I_B + I_{Rayleigh}}{2I_B} = 24.0.$$

In fact, considering the Raman scattering intensity we found that $2I_B$ represents 4% of the total scattered intensity which corresponds to

$$\frac{2I_B + I_{Rayleigh} + I_{Raman}}{2I_B} = 25.0.$$

4.3. Glass inhomogeneities

In previous work [6] we showed, from low frequency Raman scattering experiments, the shift of the Boson peak of silica towards smaller frequency when the fictive temperature decreased. Simultaneously, the Si–O–Si intertetrahedron angle, determined from the position of the 430 cm^{-1} band, increased and was correlated with a decrease of the macroscopic density [15]. The Boson peak is interpreted in the model of Duval [16,7] as being due to domains with nanometer dimensions – nanodomains – resulting from fluctuations of elastic constants. The shift of the Boson peak due to decrease of the fictive temperature is then linked to a decrease of a local sound velocity corresponding to a change of the local elastic constant inside the domains.

The Rayleigh experiments also demonstrate the inhomogeneity of pure silica, but corresponding to density fluctuations with typical sizes smaller than the wavelength of light [8]. Both types of inhomogeneities, density fluctuations and elastic fluctuations in nanodomains, are affected by fictive temperature but are likely different. Further research is necessary to achieve a full description of the glass structure but our results are consistent with a structure for a simple glass, where regions of density fluctuations are separated by smaller domains with nanometer dimensions, the former corresponding to Rayleigh scattering, the latter corresponding to low frequency anomalies (Boson peak, heat capacity excess, density of states excess).

5. Conclusion

For their complete quantitative description, light scattering experiments must take into account both elastic and inelastic phenomena i.e., Rayleigh, Raman, and Brillouin mechanisms. We show that both are affected by fictive temperature, which is determined by the frozen structure of the glass. In pure silica, the Rayleigh line decreased when fictive temperature decreased whereas the Boson peak shifted to lower frequencies. These changes are attributed to the change of two parts in the structure of the glass: larger domains of density fluctuations (Rayleigh scattering) and nanodomains corresponding to elastic fluctuations (Boson peak).

References

[1] P.H. Gaskell, D.J. Wallis, Phys. Rev. Lett. 76 (1996) 66.
[2] P.H. Gaskell, J. Non-Cryst. Solids 222 (1997) 1.
[3] P.H. Gaskell, Glass Phys. Chem. 24 (1998) 180.
[4] B. Champagnon, C. Chemarin, E. Duval, XVIII Int. Conf. on Glasses, San Francisco, 1998.
[5] C. Chemarin, B. Champagnon, J. Non-Cryst. Solids 243 (1999) 281.
[6] C. Chemarin, B. Champagnon, G. Panczer, J. Non-Cryst. Solids 216 (1997) 111.
[7] L. Saviot, E. Duval, N. Surotsev, J.F. Jal, A.J. Dianoux, Phys. Rev. B 60 (1999) 18.
[8] J. Schroeder, in: M. Tomozawa, R. Doremus (Eds.), Treatise on Materials Sciences and Technology, vol. 12, Academic Press, New York, 1977, p. 157.
[9] S. Todoroki, S. Sakaguchi, J. Ceram. Soc. Jpn 105 (1997) 377.
[10] K. Saito, H. Kakiuchida, A.J. Ikushima, J. Appl. Phys. 84 (1998) 3107.
[11] K. Saito, H. Kakiuchida, A.J. Ikushima, J. Non-Cryst. Solids 222 (1997) 329.
[12] S. Sakaguchi, S. Todoroki, T. Murata, J. Non-Cryst. Solids 220 (1997) 178.

[13] A. Agarwal, K.M. Davis, M. Tomozawa, J. Non-Cryst. Solids 185 (1995) 191.
[14] F.L. Galeener, J. Non-Cryst. Solids 5 (1970) 123.
[15] R. Brückner, J. Non-Cryst. Solids 5 (1970) 123.
[16] E. Duval, A. Boukenter, T. Achibat, J. Phys.: Condens. Matter 2 (1990) 10227.